

ASTER Observations of the Spectral Emissivity over New Mexico

Thomas Schmugge, Andrew French, Jerry Ritchie, Mark Chopping and Al Rango
USDA Hydrology and Remote Sensing Lab, Beltsville, MD 20705, USA
Tel:301-504-8554, FAX:301-504-8931, email: schmugge@hydrolab.arsusda.gov

ABSTRACT

On several days in 2000 & 2001 the Advanced Spaceborne Thermal Emission and Reflection radiometer (ASTER) on the Terra satellite obtained data over the Jornada Experimental Range test site along the Rio Grande river and the White Sand National Monument in New Mexico. ASTER has 14 channels from the visible (VNIR) through the thermal infrared (TIR) with 15 m resolution in the VNIR and 90 m in the TIR. The overpass time is approximately 11 AM (MST). With 5 channels between 8 and 12 μm these multispectral TIR data from ASTER provide the opportunity to separate the temperature and emissivity effects observed in the thermal emission from the land surface. Ground measurements during these overflights included surface temperature, vegetation type and condition and limited surface emissivity measurements. Preliminary results indicate good agreement between ASTER emissivities and ground measures. Analysis of earlier aircraft data has shown that the multispectral TIR data are very effective for estimating both the surface temperature and emissivity. These results will be compared with those obtained from the ASTER data for this site. With multispectral thermal infrared observations provided by ASTER it is possible for the first time to estimate the spectral emissivity variation for these surfaces on a global basis at high spatial resolution.

Keywords: Thermal infrared, emissivity, ASTER, remote sensing, Terra, gypsum.

1. INTRODUCTION

Knowledge of the surface emissivity is important for determining the radiation balance at the land surface. For heavily vegetated surfaces there is little problem since the emissivity is relatively uniform and close to one. However, for arid lands with sparse vegetation the problem is difficult because the emissivity of the exposed soils and rocks is highly variable. This is shown in Figure 1 where laboratory measurements of emissivity for several relevant soils are presented. In particular note the strong variations of emissivity in the 8 to 9 μm region. The data we will present are early ASTER data acquired over the Jornada Experimental Range and the White Sand National Monument in New Mexico on May 12, 2001. The Jornada site is typical of a desert grassland where the main vegetation components are grass and shrubs.

The thermally emitted radiance from any surface depends on two factors: 1) the surface temperature, which is an indication of the equilibrium thermodynamic state resulting from the energy balance of the fluxes between the atmosphere, surface and the subsurface soil; and 2) the surface emissivity which is the efficiency of the surface for transmitting the radiant energy generated in the soil into the atmosphere. The latter depends on the composition, surface roughness, and physical parameters of the surface, e.g. moisture content. In addition, the emissivity generally will vary with wavelength for natural surfaces. Thus to make a quantitative estimate of the surface temperature we need to separate the effects of temperature and emissivity in the observed radiation. The Temperature Emissivity Separation (TES) algorithm is used to extract the temperature and 5 emissivities from the 5 channels of ASTER data. TES makes use of an empirical relation between the range of observed emissivities and their minimum value. This approach will be demonstrated with data acquired over the Jornada Experimental Range in New Mexico.

2. JORNADA SITE

The Jornada Experimental Range lies between the Rio Grande flood plain (elevation 1190 m) on the west and the crest of the San Andres mountains (2830 m) on the east. The Jornada is 783 km^2 in area and is located 37 km north of Las Cruces, New Mexico on the Jornada del Muerto Plain in the northern part of the Chihuahuan Desert. The larger Jornada del Muerto basin is typical of the Basin and Range physiographic province of the American Southwest and the Chihuahuan Desert [1].

Three specific sites in the Jornada were chosen for intensive studies. Sites were selected to represent grass, shrub (mesquite), and grass-shrub transition areas. The grass site is in a fairly level area where black grama dominates and encompasses an enclosure where grazing has been excluded since 1969. Honey mesquite on coppice dunes dominates the shrub site. The dunes vary in height from 1 to 4 m with honey mesquite bushes on each dune. Bare soil dominates the lower areas between these coppice dunes with most of this area covered by a darker soil with a consolidated crust. However a portion of the interdunal area is covered by a bright quartz rich sand. Samples of these two soils were taken to the Jet Propulsion Laboratory for measurements of their emissivity spectra. The results are shown in Figure 1 along with the ASTER spectral response functions and the emissivity spectra for the gypsum sand from the White Sands area. It is clear that there will be a variation of the emissivity for the 5 ASTER channels for these soils with the shorter wavelength ones ($8 < \lambda < 9.5\mu\text{m}$) having noticeably lower emissivities.

3. ASTER

ASTER [2] has 5 thermal infrared channels between 8 and 12 μm as seen in Figure 1. The central wavelengths of the channels 10 to 14 are: 8.29, 8.63, 9.08, 10.66 and 11.29 μm . These channels have a spatial resolution of 90 m. The data we present were acquired at 18:06 GMT or 11:06 MST on May 12, 2001. The scene is cloud free and covers the Jornada site in the southwest corner and White Sands about 50 km to the northeast. In addition to the ASTER coverage, there was also an aircraft flight with the MODIS/ASTER simulator on May 12, 2001, roughly coincident with a satellite overpass but these data have not been analyzed as yet.

3.1 Temperature Emissivity Separation

The radiance at the satellite is given by

$$L_j(\text{surf}) = (L_j(a/c) - L_j(\text{atm } \downarrow)) / \tau_j \quad (1)$$

where the values of τ_j and $L_j(\text{atm } \downarrow)$ can be calculated using an atmospheric radiative transfer model, e.g. MODTRAN-4, with nearby radiosonde data. The latter were obtained from the 00 GMT NOAA sounding at El Paso. The profile was adjusted for the surface temperature and humidity conditions. The remaining problem is to relate these radiances to the surface emissivity in the 5 channels without direct knowledge of the temperature, T_{grd} using the relation:

$$L_j(\text{surf}) = \epsilon_j BB_j(T_{\text{grd}}) + (1 - \epsilon_j) \cdot L_j(\text{atm } \downarrow) \quad (2)$$

where $BB(T)$ is the Planck equation for the radiation from a black body.

Equation 2 indicates that if the radiance is measured in n spectral channels, there will be $n+1$ unknowns: n emissivities and the unknown surface temperature. The equations described by a set of radiance measurements in n spectral channels is thus under determined, and additional information is needed in order to extract the temperature and emissivity information. Using an empirical relation between ϵ_{min} and $\Delta\epsilon$, Gillespie *et al.* [3] developed the Temperature Emissivity Separation (TES) algorithm for use with ASTER data. The estimated kinetic temperature, T , is taken to be the maximum T estimated from the radiances for the n spectral channels calculated from equation 2 using an assumed emissivity value, ϵ (typically 0.98). Relative emissivities, β_j are found by ratioing the acquired radiance data (L_j), to the average of all channels:

$$\beta_j \equiv \frac{L_j / L_{BB}(\lambda_j, T)}{\bar{L} / \bar{L}_{BB}} \quad (3)$$

where the individual L_j are corrected for the effects of both the upwelling and downwelling atmospheric radiation. In principle β_j may range widely, however, since the emissivities are generally restricted to 0.7-1.0, the ratioed values are restricted to 0.7-1.4. The β_j values provide a temperature independent index which can be matched against β_j values calculated from laboratory/field measurements of natural materials. In the TES method the max-min difference ($MMD = \max(\beta_j) - \min(\beta_j)$) is related to the minimum emissivity, ϵ_{min} . From laboratory measurements of emissivities [4] the relationship between ϵ_{min} and MMD was found to be:

$$\epsilon_{min} = 0.994 - 0.687 * MMD^{0.737} \quad (4)$$

and can be used to calculate the emissivities from the β spectrum:

$$\epsilon_j = \beta_j \left(\frac{\epsilon_{min}}{\min(\beta)} \right) \quad (5)$$

The β_j are determined from the measured surface radiances L_j . From these ϵ_j a new temperature can be obtained. The process is repeated until the results converge and usually occurs after 2 or 3 iterations. A limitation of the method is that the smallest value of MMD is determined by instrument noise and the quality of atmospheric correction. This will affect the maximum ϵ that will be observed in the scene. The approach has been successfully demonstrated with data from multispectral thermal infrared data from aircraft platforms in HAPEX-Sahel[5] and for this site [6].

4. RESULTS AND CONCLUSIONS

The results of TES being applied to the May 12, 2001 scene over the Jornada and nearby White Sands are presented in Figure 2 for channels 11 and 12. We note that there is considerable variation of the emissivity over the scene, from less than 0.8 to about 0.98 for the 2 channels shown. If we had plotted one of the longer wavelength channels, i.e. 13 or 14, the scene would have been completely white using the same gray scale. The interesting feature for these two channels is the difference in emissivity for the White Sands area at the upper right. For channel 11, $\lambda = 8.63 \mu\text{m}$, the region is darker i.e. $\epsilon < 0.75$, while for channel 12 the region is much brighter with $\epsilon > 0.85$. This is as expected from Figure 1 where the dip in emissivity for gypsum is centered on the response function for channel 11. Histograms for the 5 channels are presented in Figure 3. The 3 shorter wavelength channels have a much wider range in emissivities, from < 0.85 to about 0.98, while the longer wavelength channels, 13 and 14, have much narrower distributions, from 0.94 to 0.98.

The radiances for a 2 by 2 pixel area (~ 180 by 180 m) from White Sands were analyzed and the results are presented in Figure 4, filled and open circles. The ASTER results show excellent agreement with the laboratory results. The latter were obtained for each ASTER channel by integrating the product of the ASTER response and gypsum emissivity curve shown in Figure 1. The agreement is particularly clear for the low emissivity in the $8.6 \mu\text{m}$ channel.

Also shown in Figure 4 are results for a 2 by 2 pixel area from the grass site at the Jornada, the filled and open squares. Again the agreement between the ASTER results and those calculated from the lab spectra is very good. This is a little surprising because there is generally a mix of bare soil and senescent vegetation at this site so that we would have expected to see a flatter spectral response due to the vegetation. Another interesting result is the lack of variation (< 0.01) between the two sites for the long wavelength channels.

The results for the mesquite site are given in Figure 5. In this case there is larger difference between the lab results and the ASTER results, e.g. 0.05 for the $8.29 \mu\text{m}$ channel. At this site we made field measurements with a CIMEL 312 [7] radiometer which has approximately the same 5 spectral channels as ASTER. The CIMEL results also disagree with the lab calculations and we suspect that this may be due to the fact the lab measurements were made on a powdered sample of the soil while the field measurements were done on the consolidated surface. The other surprising thing is that the effects of the light sand with its low emissivity at $8 - 9 \mu\text{m}$ and the vegetation of the mesquite bushes are not apparent.

These results indicate that the TES algorithm appears to work as well with the data from space as it did with the aircraft data presented earlier [5],[6]. This is encouraging for the application of the technique for mapping emissivity over large areas.

ACKNOWLEDGMENT

This research was supported by the ASTER project of NASA's EOS-Terra program. The laboratory emissivity measurements were made by Cindy Grove of the Jet Propulsion Laboratory.

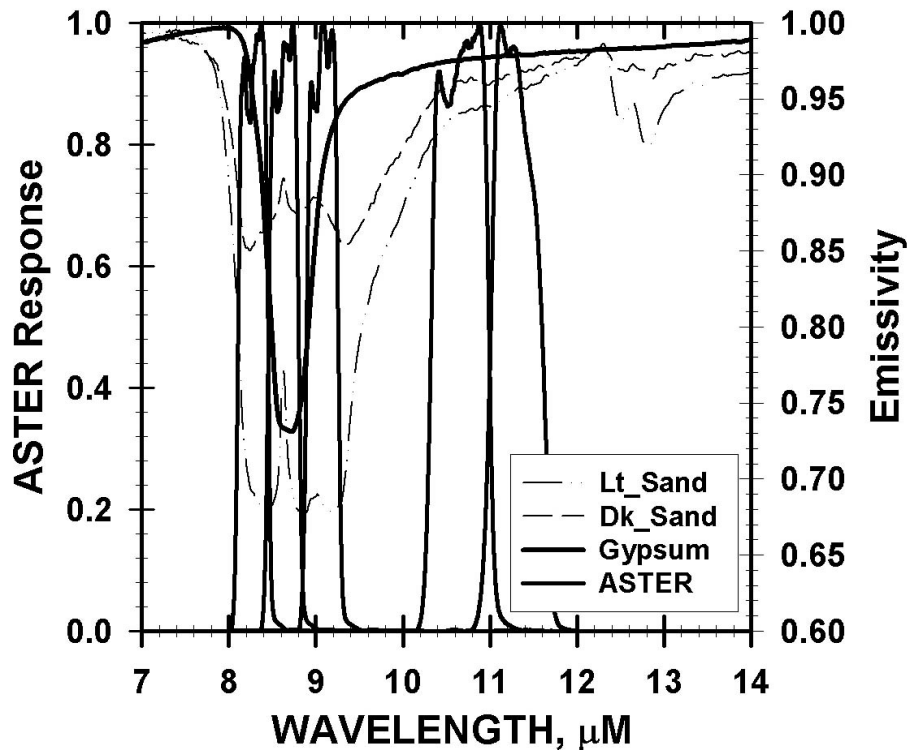


Figure 1: Plots of spectral emissivity for 3 soils from New Mexico and the response functions for the 5 ASTER channels, with channel 10 on the left and 14 on the right.

REFERENCES

- [1] K.M. Havstad, W.P. Kustas, A. Rango, J. Ritchie, and T.J. Schmugge, "JORNADA EXPERIMENTAL RANGE: A Unique location for remote sensing experiments to validate EOS satellite systems and to understand the effects of climate change in arid environments," *Remote Sensing of Environment*, **74**, pp. 13 - 25, 2000.
- [2] Y. Yamaguchi, A. B. Kahle, H. Tsu, T. Kawakami, and M. Pniel, "Overview of Advanced Spaceborne Thermal Emission and Reflection Radiometer (ASTER)," *IEEE Transactions on Geoscience and Remote Sensing*, **36**, pp. 1062-1071, 1998.
- [3] A. Gillespie, S. Rokugawa, T. Matsunaga, J. S. Cothorn, S. Hook, and A. B. Kahle, "A temperature and emissivity separation algorithm for Advanced Spaceborne Thermal Emission and Reflection Radiometer (ASTER) images," *IEEE Transactions on Geoscience and Remote Sensing*, **36**, pp. 1113-1126, 1998.
- [4] J. W. Salisbury and D. M. D'Aria, "Emissivity of Terrestrial Materials in the 8-14 μm Atmospheric Window". *Remote Sensing Environment*, **42** :83-106, 1992.
- [5] T.J. Schmugge, S.J. Hook, and C. Coll, "Recovering surface temperature and emissivity from thermal infrared multispectral data," *Remote Sensing of Environment*, **65**, pp. 121-131, 1998.
- [6] T. Schmugge, A. French, J.C. Ritchie, A. Rango, and H. Pelgrum, "Temperature and emissivity separation from multispectral thermal infrared observations," *Remote Sensing of Environment*, **78**, pp. xx-yy, 2001.
- [7] M. Legrand, C. Pietras, G. Brogniez, M. Haeffelin, N.K. Abuhassan and M. Sicard, "A High-accuracy multiwavelength radiometer for in situ measurements in the thermal infrared. Part 1: Characterization of the instrument," *Journal of Atmospheric & Oceanic Technology*, **71**, pp. 1203-1214, 2000.

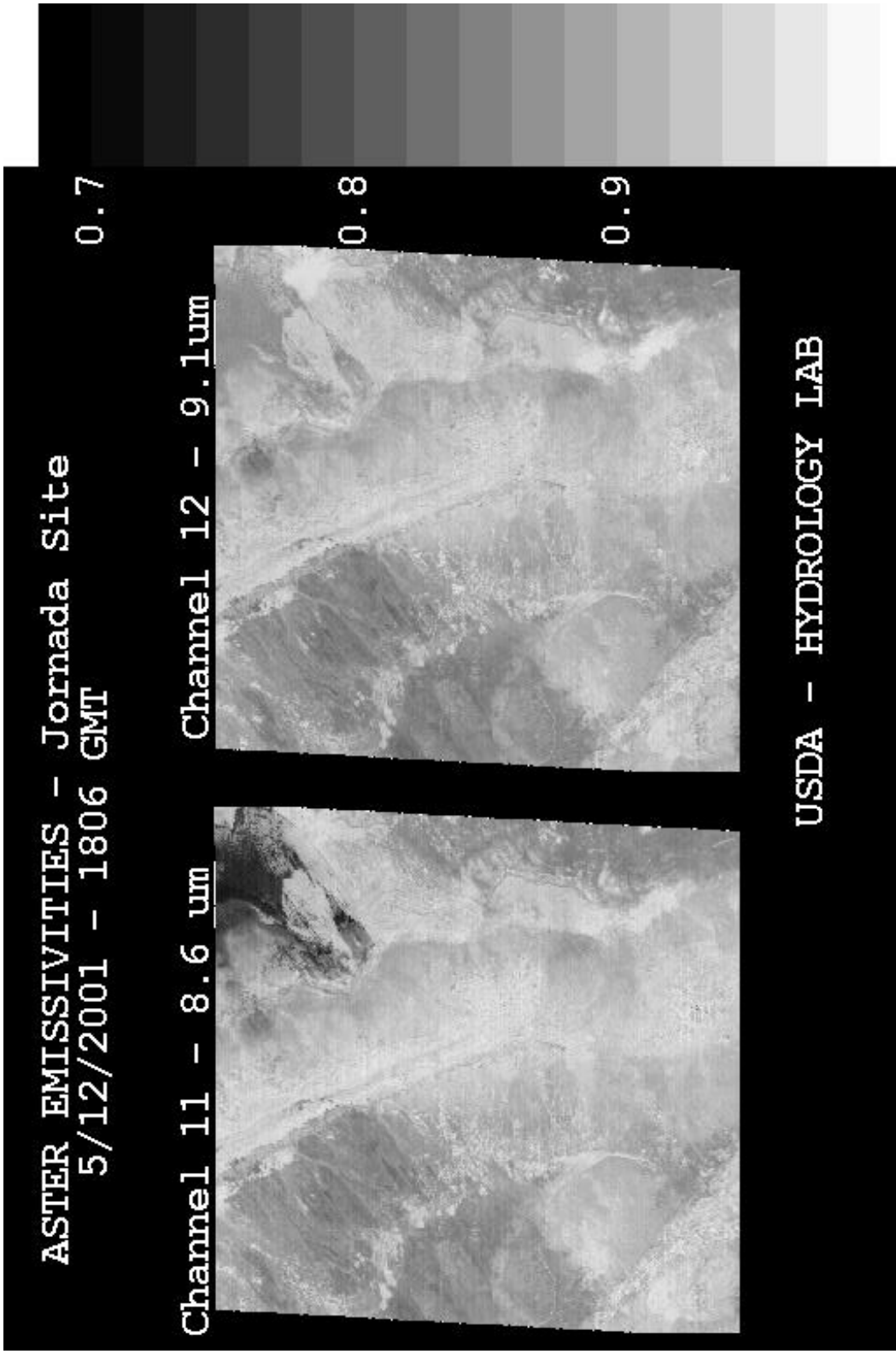


Figure 2. Maps of emissivities for two of the ASTER channels. The Jornada Experimental Range is at the lower left of the images and the White Sands is lower emissivity area at the upper right.

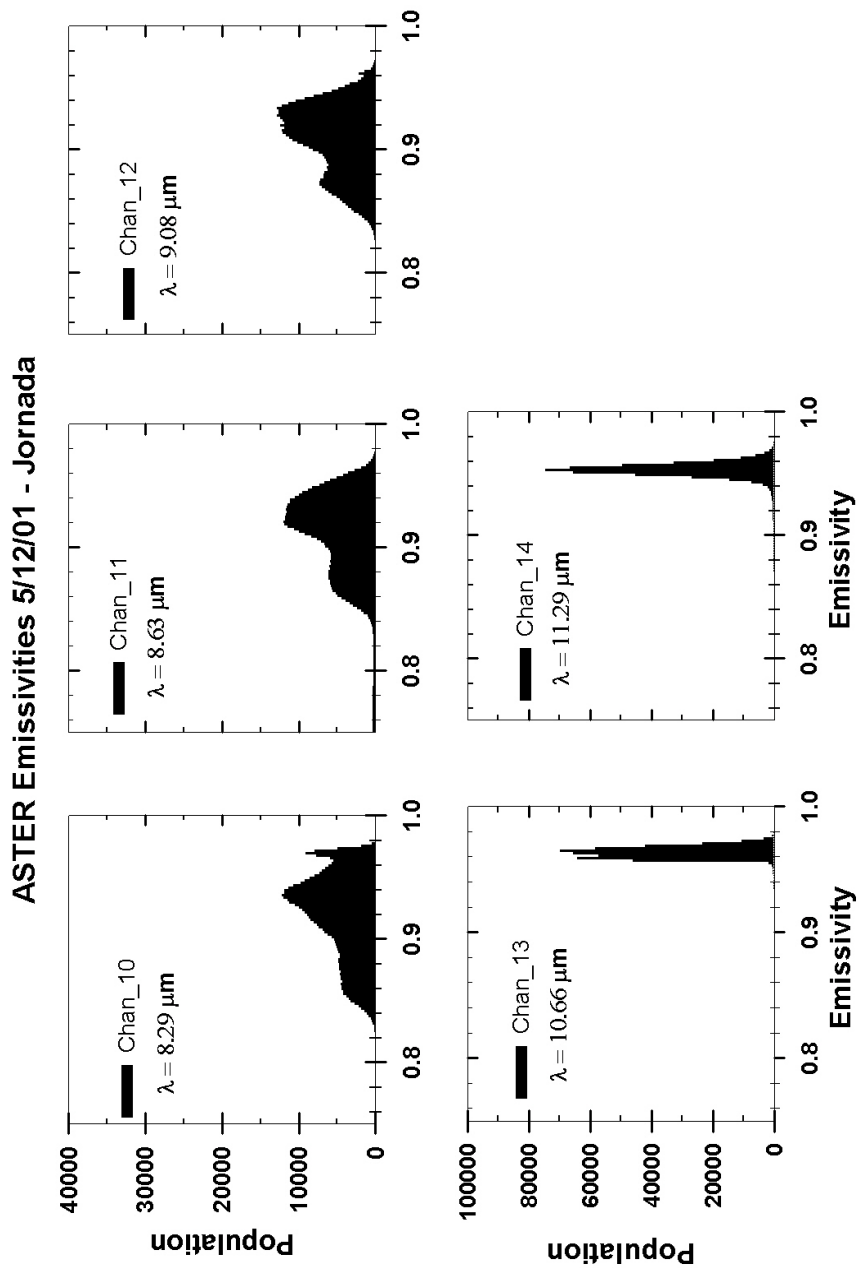


Figure 3. Histograms of the emissivities for the 5 ASTER channels for the May 12, 2001 scene which covers the Jornada Experimental Range and the White Sands National Monument. Note the difference in vertical scales between the short wavelength channels at the top and the two long wavelength channels in the bottom panels.

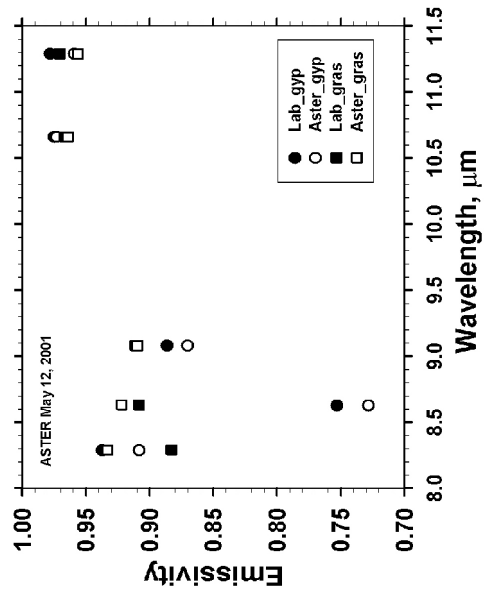


Figure 4. ASTER emissivity results for a gypsum site, the circles, at White Sands and the grass site, the squares, at the Jornada.. The open symbols are the ASTER results and the closed are the lab results.

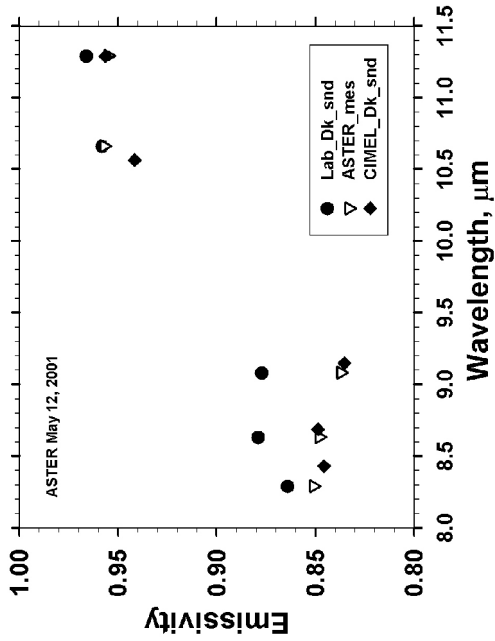


Figure 5. ASTER emissivity results for the mesquite site at the Jornada, again the open symbols represent the ASTER results.